ZIBELINE INTERNATIONAL™ PUBLISHING

ISSN: 2521-2915 (Print)
ISSN: 2521-2923 (Online)
CODEN: PJGABN

Pakistan Journal of Geology (PJG)

DOI: http://doi.org/10.26480/pjg.01.2025.12.19

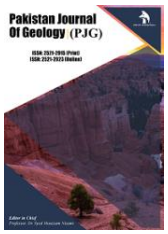

RESEARCH ARTICLE

APPLICATION OF GEO-ELECTRICAL TECHNIQUES FOR GROUNDWATER POTENTIAL DELINEATION IN MASHIJI AND ITS ENVIRON, MALUMFASHI NORTHWEST NIGERIA

Shuaibu A.M[a], Shehu S Abdulmalik[b], [a]Okiyi I.M[a]

[a]Department of Geology, Faculty of Science, Federal University Lokoja, Kogi State.
[b] Department of Geological Sciences, Faculty of Science, Federal University Gusau, Zamfara State.
**Corresponding author's email: mahalkufr@gmail.com*

ARTICLE DETAILS

Article History:

Received 10 January 2025
Revised 15 February 2025
Accepted 26 February 2025
Available online 13 March 2025

ABSTRACT

Thirty-five (35) vertical electrical soundings (VES) were conducted to assess the groundwater potential of Mashiji and its surroundings using the Schlumberger configuration with a maximum current electrode of 100 m and an Ohmega resistivity meter. The data were analyzed using IPI 2win software. The research region is dominated by the HK curve type (20%), followed by the H, HA, and A curve types (60%), and KH, KA, AK, and KA curve types (20%). Groundwater potential aquifer production zones were identified using geoelectric techniques. Weathered and fractured layers make up the majority of the aquifer zones in the research region. The granitic environment of the study area is separated into four subsurface strata, according to the geoelectric sections: top soil, clayey laterite, weathered basement, fractured basement, and, occasionally, fresh basement. These horizons have thicknesses ranging from 0.48 to 1.61 m, 1.55 to 13.7 m, 2.75 to 35.7 m, 12.2 to 75.3 m, and 17.8 to ->7 m, in that order. In a metasediment environment, geoelectric sections revealed that the area is made up of four geoelectric layers: top soil, clayey lateritic soil, quartzite/schist, weathered basement, and, in some cases, fresh basement. The thicknesses of these horizons are 0.40 - 1.34m, 1.7 - 8m, 3.63 - 28m, 4,374 - 34.9m, 4.9 - 59.4m, and 25.2 - 60m. The fractured/overburden geospatial maps of the study area indicated diverse groundwater potentials depending on geological conditions. The weathered and fractured thicknesses in the granite environment range from 2.75 to 35.7 m and 12.2 to 75.3 m, respectively, while in the metasediment environment, the weathered basement thickness is 4.374 to 34.9 m, and the fractured layer thickness varies from 4.9 to 59.4 m.

KEYWORDS

Resistivity survey, vertical electrical sounding, geoelectrical section, weathered or fractured aquifer, groundwater potential.

1. INTRODUCTION

The insufficient supply of potable pipe-borne water in Malumfashi town as a whole, as well as the lack of public water supply in Mashiji and surrounding areas, are major concerns. Water scarcity in Kutosheka and Mashiji in Katsina State, is a concern, particularly during the dry season. Many boreholes in these regions of Malumfashi collapse during the dry season, with few exceptions. At short depths, hand-dug wells can be used to extract groundwater trapped in weathered granite or schist in the earth's crust (Olurufemi and Fasuyi, 1993). The yield is often low and varies according to the season and climate (Bala and Ike, 2001; Alisiobi and Ako, 2012; Obuobie and Barry, 2010). A study states that hand-dug wells are frequently found in valley areas where seepage occurs and along drainage lines where the weathered zone is frequently thick (Oluwa, 1967).

Nigerian aquifer distribution can be broadly divided into two systems: sedimentary aquifers and basement fractured aquifers. A group researcher discovered that the formation of thick soil overburden (overburden aquifers) or the existence of water-holding fractures (fractured crystalline aquifers) determine the groundwater availability in regions covered by crystalline basement rocks (Aboh, 2001; Nur and Kujir, 2006; Al-Garni, 2009; Ariyo, 2010; Nur and Ayuni, 2011; Shuaibu, 2024). According to a study, the lack of water supplies is one of the biggest environmental issues facing rural populations in northern Nigeria (Kwari, 2015). The primary source of water for household and animal use in the majority of northern Nigerian rural villages is a hand-dug well.

Rocks from the Precambrian Basement Complex, which have limited porosity and permeability, underlie the research area. Areas with heavy overburden covering fractured zones—which are frequently identified by comparatively low resistivity values—have the largest groundwater production in these types of terrains (Shuaibu et al., 2022). Such zones are good places to drill wells for portable, pollutant-free groundwater production (Alabi et al., 2010). This community's residents are prone to water-borne illnesses because they usually rely on a variety of water sources, including hand-dug wells and streams, which are notoriously polluted (Ologe et al., 2014).

In basement terrains, a variety of geophysical techniques have been effectively used to search for ground water. These techniques include, among others, electrical, magnetic, and electromagnetic. The electrical resistivity approach has been the most popular of these techniques for investigating groundwater (Shuaibu, 2024). Because of its ease of use and dependability, the VES (Vertical Electrical Sounding) electrical resistivity method is frequently employed for depth sounding (Olawuyi and Abolarin, 2013). Since the electrical resistivity of most rocks depends on the amount of water in their pore spaces, the distribution of those pores, and the salinity of the water in those spaces, it is used to assess the vertical

Quick Response Code	Access this article online	
	Website: www.pakjgeology.com	DOI: 10.26480/pjg.01.2025.12.19

Cite The Article: Shuaibu A.M, Shehu S Abdulmalik, Okiyi I.M (2025). Application of Geo-Electrical Techniques for Groundwater Potential Delineation in Mashiji and Its Environ, Malumfashi Northwest Nigeria. *Pakistan Journal of Geology, 9(1): 12-19*.

variation of electrical resistivity beneath the earth's surface (Oladunjoye and Jekayinfa, 2015).

The current investigation is aimed at giving fundamental information regarding the groundwater potential of Malumfashi metasedimentary Province utilizing Vertical Electrical Sounding (VES) with the idea of fulfilling the following purpose. 1. To conduct detail vertical electrical sounding in order to delineate aquiferous zone in terms of its thickness/depth of aquifer units. 2. Define the water-bearing zone of the area.
Borehole drilling businesses operating in the research area can benefit from the study's findings. Knowing the location of the aquifer thickness/depth can assist eliminate the problem of failed boreholes in the research areas.

2. Geology of The Study Area

The mapped area is located in Katsina state's Malumfashi local government area, which is part of the Malumfashi topographic sheet 79 NW. On a scale of 1:25,000, the area is 40 km^2 and is bordered by latitudes N11º49'00" and N11º53'00" and longitudes E7º34'00" and E7º37'00" (Figure 1). The schists in the study region are found in northwest Nigeria, in the Malumfashi schist belt. Schists, migmatite-gneiss, quartzite, and Pan-African granite make up the majority of this belt, which is one of the twelve schist belts that have been found in Nigeria to date. Pegmatite and aplite are minor lithologies. The main constituents of the Malumfashi schist belt, according to a study, are phyllite interbedded with thin quartzites and muscovite and biotite schist (McCurry, 1976).

The pelitic rocks have a high concentration of quartz and quartz-tourmaline veins, together with trace levels of feldspathic and graphitic schists. Most interbedded quartzites are very large. Well-bedded quartzite units, sometimes tens of meters thick, are also present. Minor rocks include spessartite quartzite, calc-silicate rocks, and anthophyllite cordierite schist. Uneven bands of amphibolite can occasionally form; the largest occurrence is just around 12 meters thick. A lithological study between the Kushaka and Malumfashi schist belts was done (Grant, 1978). The fact that (1) the quartzites are detrital rather than chemically precipitated iron-silica formations and (2) basic igneous rocks are of far lesser significance are two other important differences. The rocks are a sequence of fine-grained muds and sands that are quite well-differentiated. The size and shape of the Zungeru-Birnin Gwari Schist belt are very similar to those of the Malumfashi belt (Grant, 1978).

The formation of Nigeria's schist belts has been explained by a number of theories. Some researcher argues that the genesis of the schist belts is due to ensialic mechanisms (McCurry, 1971). While in other studies, they advocated evolution through ensimatic processes, some researchers suggested the creation of rift zones when sufficient extension produced small basin favored formation through both ensialic and ensimatic processes (Ajibade and Wright, 1989; Ogezi, 1981; Holt, 1982). The Kazaure Schist Belt is sedimentary in origin and was most likely created by the metamorphism of shale greywacke, according to geochemical characteristics described (Danbatta, 2001).

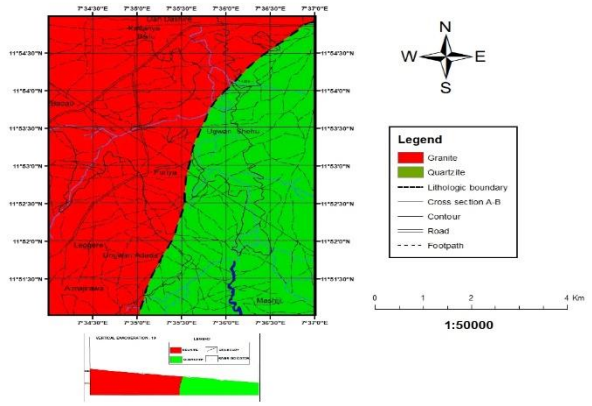

Figure 1: Geological Sketch of the Study Area

3. Materials and Method

Resistivity determinations are usually made by injecting a specified amount of electric current into the ground through a pair of current electrodes and then, with the aid of a pair of potential electrodes, measure the potential difference between any two points at the surface caused by the flow of the electric current in the subsurface. From the measured current (I) and the voltage (V) values, the ensuing resistivity is determined. Geo-electrical investigations involving resistivity survey using Schlumberger array was conducted around 7 profiles in the study area, each profile carrying 5 station making it to be 35 station point, using instruments Ohmega resistivity meter with all other accessories like wires reel for current and potentials, four electrodes and connections wires.

Others include cutlass, hammer, tape, paper, umbrella and of course recording sheets. Twenty three 23 VES out of 35 were conducted at granitic environment while 12 VES were conducted within quartzite/schistose environment with maximum current electrode separations of 100m (The potential electrodes remain fixed and the current electrodes were expanded simultaneously about the center of the spread. The results were interpreted using IPI 2win software, and the geo-electrical sections were plotted with the help of Autocard. The maximum electrode separation used was AB/2 = 100m, and the maximum potential electrode spacing was MN/2 = 5m. These electrodes are typically arranged in a straight line, with the potential electrode placed in between the current electrodes, as shown in Figure 2.

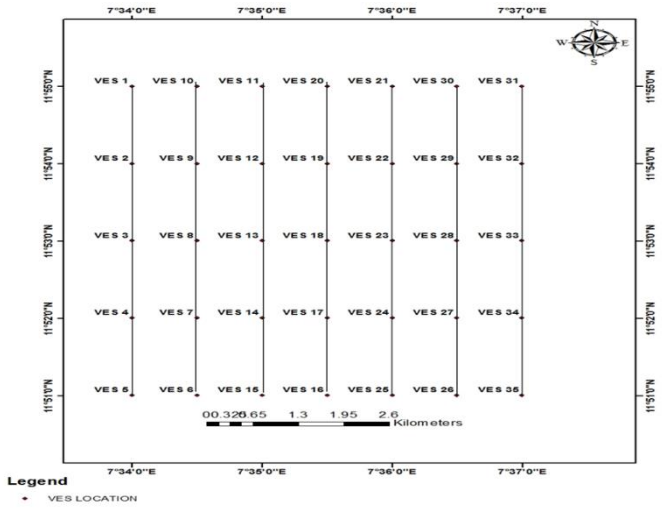

Figure 2: Schematic Diagram of Profile Line of the Survey within the Study Area

The 2D electrical resistivity data was gathered using the ABEM Lund Imaging system, which consists of a Terrameter SAS 4000 enhanced by an automated multi-electrode system. Due to its high signal-to-noise ratio and unit electrode spacing of 5 m, the Wenner32SX protocol was used for Wenner-CVES roll-along measurement using two cables. Figure 2 displays, to scale, the profile lines (P1–P8) that were used to collect the data. The reservoir's southern and northern flanks are occupied by P1–P4 and P5–P8, respectively. The RES2DINV computer tool was used to evaluate the raw data acquired for this investigation, including measured apparent resistivity (Geotomo Software, 2001). It takes a 2D subsurface model to analyze a 2D piece of data.

The subsurface is divided into numerous rectangular sections by the program's 2D model. The resistivity of the rectangular blocks is then estimated by the method, producing an apparent resistivity pseudosection (calculated apparent resistivity) that agrees with the actual measurement. The finite-difference forward modeling program was used to determine the apparent resistivity values. To increase the accuracy of the calculated apparent resistivity in the forward modeling, a relatively dense mesh grid with four nodes per unit electrode spacing was employed, albeit at a computational expense in terms of time. Block thickness increased by 13% with each deeper layer after the initial layer, which was set at 0.5 times the unit electrode spacing.

Every inversion technique aims to create a subsurface model whose response aligns with the observed data. The measured apparent resistivity is the data in the cell-based method of the RES2DINV program, whereas the model parameters are the resistivity values of the model blocks. By iteratively modifying the resistivity of the model blocks, the optimization method basically aims to minimize the discrepancy between the computed and observed apparent resistivity values. This difference is measured by the root-mean-squared (RMS) error. The "best" model is typically the one at the iteration where the RMS error does not change much, which happened in our case between the fifth and seventh iterations.

4. Results and Discussion

Tables 1 and 2 provide a summary of the interpreted layer parameters for each VES station based on the 1D-resistivity curves. The investigation's findings were similarly presented in the form of geo-electrical divisions for easier comprehension. However, the bedrock is made up of the fracture and the new basement rocks, whereas the top soil, lateritic soil, and weathered basement are considered the overburden.

Table 1: Interpreted Layered Parameter of the Granitic Environment of the Study Area

VES location and coordinate	Layer/Curve Type	Resistivity ohm-m	Thickness (m)	Depth (m)	layer characteristics
	AK	33.3	0.678	0.678	top soil
VES 1		81.1	5.65	6.33	lateritic soil
		4808	19.0	25.3	weathered basement
		27.6			fractured basement
	A	20.9	0.479	0.479	top soil
VES 2		97.5	8.97	9.45	lateritic/weathered basement
		88594			slightly fractured/fresh basement
	KA	51.7	1.61	1.61	top soil
VES 3		433	33.8	35.4	weathered/slightly fractured
		79157			fresh basement
	HA	308	1.02	1.02	compacted top soil
VES 4		106	1.91	2.93	lateritic soil
		161	20.1	23.03	weathered/slightly fractured
		87544			fresh basement
	HA	20.6	0.8661	0.8661	clayey top soil
VES 5		296	0.666	1.55	lateritic soil
		33.9	3.07	4.62	weathered basement
		984	26.5	31.1	fractured basement
		58291			fresh basement
	HA	121	1.3	1.3	top soil
VES 6		10.6	1.45	2.75	weathered basement
		33926			slightly/fresh basement
	A	39	1.33	1.33	top soil
VES 7		107	0.966	2.29	lateritic soil
		522	15.5	17.8	weathered basement
		3614			slightly fractured/fresh basement
	AH	26.9	0.774	0.774	top soil
VES 8		15.5	3.54	4.32	lateritic soil
		2634	7.08	12.4	weathered basement
		248	7.3	19.7	fractured basement
		4243			fresh basement
	K	28.8	0.853	0.853	top soil
VES 9		89.3	13.71	14.58	lateritic soil
		18334	14.29	28.81	weathered basement
		44.1			fractured basement
	AK	1.27	0.713	0.713	clayey layer
VES 10		34.4	1.4	2.11	lateritic soil
		187	18.3	20.41	weathered basement
		67	40.3	60.71	fractured basement
	KH	44.4	2.59	2.59	top soil
VES 11		4084	7.53	10.1	lateritic soil
		1081	7.60	17.6	weathered basement
		3.81			fractured basement
	A	88.3	0.672	0.672	top soil
VES 12		9.62	6.45	6.45	lateritic soil
		1031	9.8	16.25	weathered basement
		67345			slightly fractured/fresh basement
	KH	3787	2.13	2.13	compacted lateritic soil
VES 13		36.8	8.82	8.82	clayey laterite

Table 1 (cont): Interpreted Layered Parameter of the Granitic Environment of the Study Area					
		263	5.19	16.1	weathered basement
		312	30.3	46.4	fractured basement
		7282			fresh basement
	HK	106	0.927	0.927	top soil
VES 14		15.2	1.38	2.31	clayey soil
		22809	2.62	4.93	lateritic soil
		386	12.31	17.25	weathered basement
		25.3			fractured basement
	HK	51.9	0.938	0.938	top soil
VES 15		317	0.645	1.58	lateritic soil
		22.6	5.65	7.24	clayey soil
		9651	10.57	17.81	weathered basement
		859			fractured basement
	HA	84.8	1.38	1.38	top soil
VES 16		10.8	6.35	6.35	weathered basement
		108	17.3	25.05	fractured basement
		1110			fresh basement
	HK	33.5	0.913	0.913	top soil
VES 17		248	1.2	2.11	compacted laterite
		10.9	3.71	3.71	clayey layer
		5446	6.39	12.2	weathered basement
		42.2			fractured basement
	H	103.4	1.259	1.259	sandy top soil
VES 18		38.05	6.127	7.306	lateritic soil
		1346	11.6	19	weathered basement
		298.4			fractured basement
	AK	38.8	0.529	0.529	top soil
VES 19		83.3	4.29	4.81	lateritic soil
		1170	18.8	23.7	weathered basement
		240	19.9	43.6	fractured basement
		7905			fresh basement
	H	653	2.11	2.11	compacted lateritic soil
VES 20		54.5	11.5	13.6	laterite
		2215	28.1	35.7	weathered basement
		240	39.6	75.3	fractured basement
		17051			fresh basement
	A	86.1	0.693	0.693	top soil
VES 21		8.74	7.81	8.45	clayey layer
		1071	10.2	18.65	weathered/slightly fractured basement
		4029			fresh basement
	H	164	0.518	0.518	sandy top soil
VES 22		446	4.02	4.52	compacted lateritic soil
		15.9	10.18	15.7	weathered basement
		398			fractured basement
	HA	1.71	1.26	1.26	clayey layer
VES 23		24.3	1.41	2.67	lateritic soil
		1257	3.05	5.72	Compacted laterite
		104	8.21	13.9	weathered basement
		815	20.4	34.3	fractured basement
		10442			fresh basement

From The results of the electrical resistivity survey (interpreted layer parameter) in granitic environment, four lithological sections were inferred. These are top soil, lateritic horizon, and weathered fractured basement though in some instances there are presence of fresh basement making it five lithological sections. The thickness of these horizon varies from 0.48 - 1.61m,1.55 -13.7 m, 2.75 - 35.7m, 12.2 - 75.3m and 17.8 -->75m for top soil, lateritic layer, weathered basement, fractured/fresh basement respectively within the Granitic environment. Likewise, the resistivity value ranges from 51.7 - 20.9 Ωm (top soil), 196 - 89.3 Ωm (lateritic soil), 33.9 – 221 Ωm (weathered basement), 42.2 – 240 Ωm (fractured

basement), and 5221 - 17051 Ωm (fresh basement) accordingly. The fractured layer is regarded as the aquiferous unit within this rock unit.

From the results of the geo-electrical survey (interpreted layer parameter) within the metasedimentary environment (Quartzite interbedded with schist) of the study area are presented in Table 2, five lithological sections were inferred. These are top soil, ferruginous quartzite, and weathered/fractured schist though in some instances there are presence of fresh basement making it six lithological sections. The thickness of these horizon varies from 0.40 - 1.34m,1.7 - 8m, 3.63 - 28m, 4,374 - 34.9m, 4.9 - 59.4m and 25.2 - 60m for Top Soil, Lateritic Layer, ferruginous quartzite, phyllite/schist, Weathered basement, Fractured and fresh basement respectively within the metasedimentary environment. Likewise, the resistivity value ranges from 68.6 - 71.7Ωm (top soil), 14.6 - 13.2Ωm (ferruginous quartzite), 18.2 - 134Ωm (phyllite/schist), 18.2 - 10.4Ωm (weathered basement), 95.4 - 79.1 Ωm (fractured basement), and 25.2 - 60 Ωm (fresh basement) accordingly.

Table 2: Interpreted Layered Parameter of the Quartzite/Schistose Environment of the Study Area

VES location and coordinate	Layer/Curve Type	Resistivity ohm-m	Thickness (m)	Depth (m)	layer characteristics
	KH	35.5	9.63	9.63	F-Quartzite & little top soil
VES 24		10.4	24.8	34.4	Weathered basement
		322			fractured basement
	AK	9.49	1.16	1.16	F-Quartzite materials
VES 25		14.6	0.532	1.7	F-Quartzite
		528	4.24	5.94	weathered basement
		73.3			fractured basement
	HK	83.5	0.911	0.911	top soil
VES 26		14.2	6.781	9.9	weathered Quartzite
		79	50.67	59.4	fractured basement
		323			fresh basement
	HK	71.7	1.34	1.34	top soil
VES 27		25.1	4.26	5.6	F-Quartzite
		13.4	4.56	10.2	fractured basement
		134	17.9	28	weathered phyllite
		56.5			highly fractured basement
	HK	85.5	0.853	0.853	top soil
VES 28		13.2	7.16	8	F-Quartzite
		56.2	15.3	23.3	weathered phyllite
		143	12.1	35.3	slightly fractured basement
		0.406			highly fractured basement
	H	68.6	0.40	0.40	top soil
VES 29		19.5	2.52	2.65	F-Quartzite
		13.9	2.25	4.9	weathered basement
		95.4			fractured basement
	H	318	1.9	1.9	compacted lateritic top soil
VES 30		18.2	1.14	3.03	Phyllite
		18.2	1.71	4.74	weathered basement
		18.2	19.7	24.5	highly fractured basement
		93.4			fractured basement
	H	267	0.872	0.872	compacted lateritic top soil
VES 31		37.3	5.83	6.7	F-Quartzite
		2139	5.79	12.5	weathered basement
		108			fractured basement
	KA	12.8	3.82	3.82	F-Quartzite
VES 32		72	8.15	12	weathered phyllite
		25.6	8.56	20.5	highly fractured basement
		233			fractured basement
	HK	21	2.77	2.77	Quartzite
VES 33		9.29	2.715	5.48	weathered phyllite
		21.7	13.6	25.2	fractured basement
		5481			fresh basement
	HK	57.7	3.74	3.74	F-Quartzite & top soil
VES 34		9.85	3.14	6.88	F-Quartzite
		1741	8.46	15.3	weathered basement
		0.892	24.5	39.8	highly fractured basement

Table 2 (cont): Interpreted Layered Parameter of the Quartzite/Schistose Environment of the Study Area					
		5481			fresh basement
	H	78.9	0.43	0.43	top soil
VES 35		18.9	3.06	4.49	F-Quartzite
		8.44	4.94	9.44	weathered basement
		24			highly fractured basement

An Isoresistivity maps of the overburden/fracture depth were plotted to show (Figures 3 and 4) the area with relatively low resistivity values corresponds to weathered or fractured basement and with relatively high resistivity values interpreted as fresh basement.

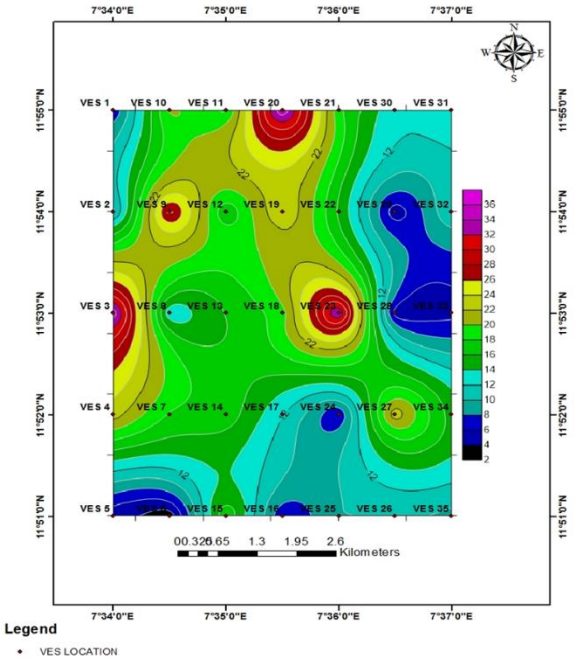

Figure 3: The isopach map of the overburden depth in the study area.

Figure 3 displays the Isopach map of the research area, which shows the depth of the overburden (down to the basement). The center, western, and northern regions of the research area are the deepest, while the southwest, south, and northeast regions are the shallowest. The area with high overburden thickness, which corresponds to basement ridges, and the area with low overburden thickness, which corresponds to basement high, are detailed in the fracture depth isopach map (Figure 4). A well fractured basement was found in the northwest portion of the study region, while a slightly or less fractured basement was found in the south-west and northeastern parts of the study area, according to the isopach map of the fractured basement displayed in Figure 4.

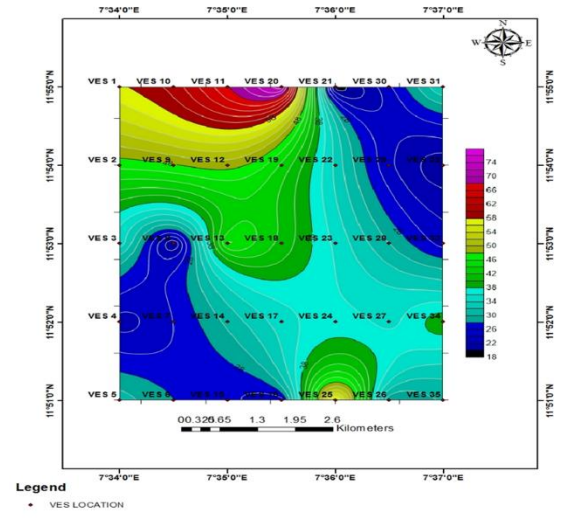

Figure 4: Isopach map of the Fractured Basement in the Study Area

The region with the largest groundwater potential was mostly produced where the fractured zone was covered by substantial overburden. Based on this claim, the maps in Figures 3 and 4 as well as Figure 1 were suitably juxtaposed, and the outcome showed that because of their high regolith thickness and weathered basement, granitic rock units are more promising for groundwater sitting than those of metasedimentary (Quartzite intercalated with schists) environments. Even yet, the groundwater potential of metasedimentary terrain tends to be comparable to that of quartzite/schistose rocks that appear fragmented.

VES from points 1 to 5 make up this geo-electric portion of profile 1 (Figure 5). The line is composed of four layers, according to the geo-electric section along profile 1. The top soil is the first layer, with a resistivity range of 20.9 to 308Ωm and a thickness range of 0.7 to 1.2 m. Station 4 has a comparatively larger thickness, while Station 5 has a relatively shallow one. With a resistivity range of 181.1 to 439 Ωm and a thickness range of 1.5 to 9.1 m, the second layer is made up of clayey laterite, which is thicker at station 2 and comparatively shallow at station 3. The third layer is a weathered basement with a thickness of 24 to 36.4 m and a resistivity range of 98 to 161 m. It is quite shallow at station 3 and has a high thickness. With a resistivity range of 8859 to 4808 Ωm, the fourth layer, which is to infinity, is the partially fractured/fresh basement rock, as shown by the reflection coefficient calculation.

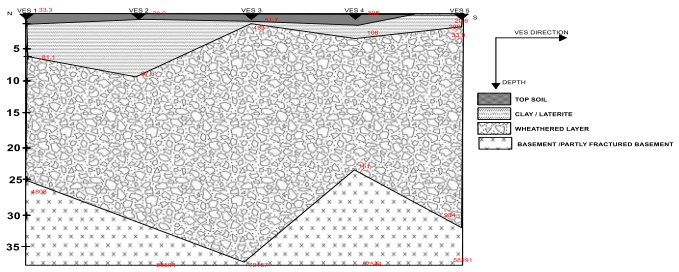

Figure 5: The geo-electric section for profile 1 of the study area

VES from points 6 to 10 make up this geoelectric segment of profile 2 (Figure 6). The resistivity top soil is the first layer, with a resistivity range of 1.2-152Ωm and a thickness range of 0.4 to 1.1 m. It is relatively thick at station 6 and relatively shallow at station 10, according to the geoelectric section along profile line 2. With a resistivity range of 107–15Ωm and a thickness range of 1.3–12 m, the second layer is made up of clayey laterite, which is thicker at station 9 and comparatively shallow at station 6. The third layer is the weathered foundation, which ranges in thickness from 24 to 36.4 m and resistivity from 98 to 161 m. Station 9 has the thickest layer, while Station 6 has the shallowest. The fourth layer which is to infinity, as revealed by the computation of the reflection coefficient is the partly fractured/fresh basement rock and has resistivity range of 3614 to 8374 Ωm.

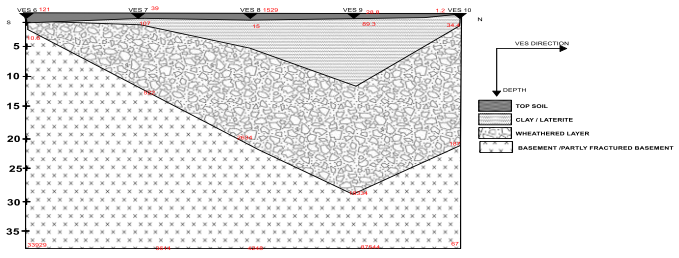

Figure 6: The geo-electric section for profile 2 of the study area

VES from points 11 to 15 make up this geoelectric segment of profile 3 (Figure 7). According to the geo-electric section along profile line 3, the line is composed of four layers. The resistivity top soil is the first layer, with a resistivity range of 9.62–378Ωm and a thickness range of 0.4–1.1m. Station 11 has a comparatively higher thickness, while Station 15 has a relatively shallow one. With a resistivity range of 10.7–408Ωm and a

thickness range of 1.6–10.4m, the second layer is made up of clayey laterite, which is thickest at station 11 and comparatively shallow at station 15. With a resistivity range of 208–2265Ωm and a thickness range of 24–36.4m, the third layer is a weathered basement. Station 14 has a high thickness, while Station 13 has a comparatively shallow thickness. A computation of the reflection coefficient reveals that the fourth layer, to infinity, is the partially fractured/fresh basement rock, with a resistivity range of 108 to 6732 Ωm.

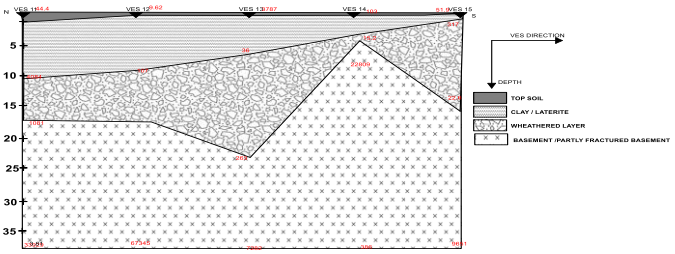

Figure 7: The geo-electric section for profile 3 of the study area

For the first profile P1, for instance, Figure 8 displays the entire collection of geoelectrical pictures (measured apparent resistivity pseudosection, computed apparent resistivity pseudosection, and the inverse model resistivity section). This profile contains around seven geoelectric segments, each of which is represented by a different hue. The degree of consistency between the computed and observed apparent resistivity pseudosections (Figure 8) reflects the dependability of the inverse model resistivity section.

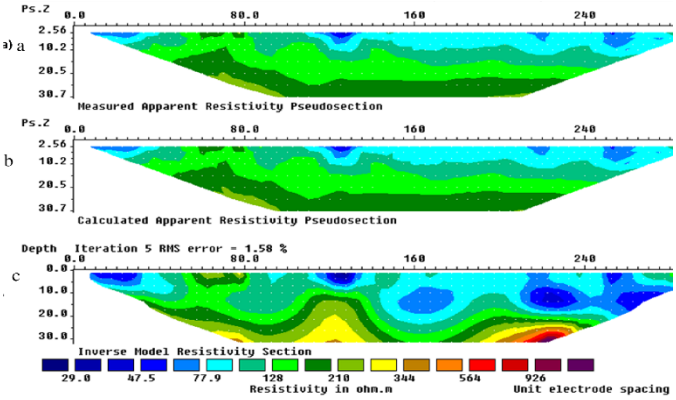

Figure 8: The data set along traverse P1, the inverse model resistivity section and the estimated and observed apparent resistivity pseudosection

Using local geology data and information from borehole logs, the inverse model resistivity section is geologically meaningfully interpreted (Shuaibu, 2024). A lithological unit-base model classification is derived (Tables 1 and 2) for the interpretation of the inverse model resistivity sections obtained by combining these data with the range of resistivity values found in the inverse model resistivity sections for all the profiles examined in this work (Figures 8 – 10). According to the classification in Tables 1 and 2, the seven geoelectric segments in the inverse model resistivity section for the first profile (Figure 8) make up three separate geologic layers.

Saturated sandy clay (with a resistivity range of 22.5 to 90 ohm-m) and saturated laterite (132 to 143 ohm-m) make up the top layer. The thickness of this layer ranges from roughly 15 meters. The extremely weathered basement, which has a thickness of roughly 5 to 12 meters, is the second stratum with a resistivity range of 126 to 295 ohm-m. The partially fractured basement is thought to be represented by the third layer of resistivity, which extends down to the depth of investigation and ranges from 80 to 125 meters. The resistivity range of the weathered basement below is the same as that of the lateritic strata close to the surface (Figure 8).

Therefore, both strata are distinguished by the depth of occurrence and the homogeneity of the geoelectric segments that comprise the weathered basement, which is an indication of in-situ chemical modification of the hard rock. Figures 9 through 10 show the remaining 2D inverse model resistivity sections along with their geologic interpretation (the opposing profiles are placed next to each other to aid in visual correlation and anomaly detection).

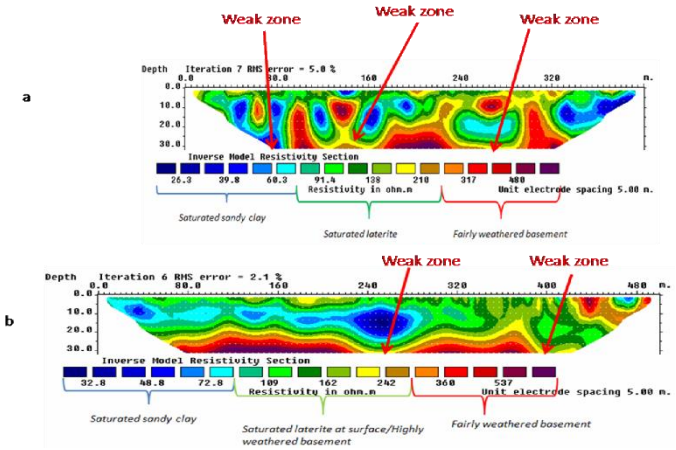

Figure 9: Along traverses P1 and P2, the Werner configuration inverted resistivity section displays the attributed lithology and anomaly of interest (weak zone within bedrock)

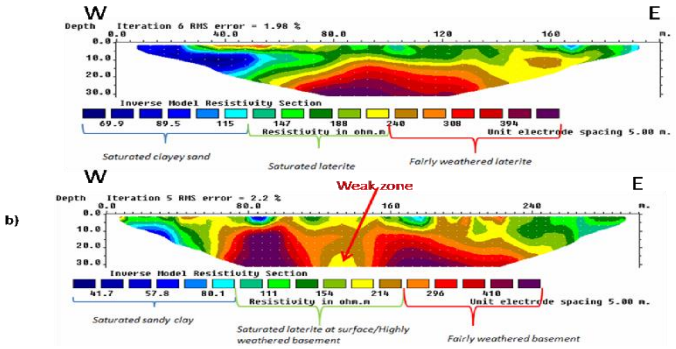

Figure 10: Along traverses P3 and P4, the Werner configuration inverted resistivity section displays the attributed lithology and anomaly of interest (weak zone within bedrock)

Under P2, the saturated clay range of 29 to 64 ohm-m is sporadically dispersed. With a length of roughly 80 m and a thickness of roughly 1.1 m, whereas saturated laterite, which has a range of values between 85 and 160 ohm-m, takes up a larger percentage of the surface layer. The basement beneath both profiles is severely weathered and fractured, as seen by the moderate resistivity layer that lies beneath the sandy clay and lateritic top layer. This layer ranges from 132 to 310 ohm-m beneath P1 and from 205 to 294 ohm-m beneath P2.

5. Conclusion

The application of resistivity surveys for groundwater potential delineation in Mashiji and its environs has provided valuable insights into the subsurface hydrogeological characteristics of the area. Through the interpretation of thirty-five (35) Vertical Electrical Sounding (VES) data, the study successfully identified key aquifer-producing zones, primarily controlled by weathered and fractured basement formations. The resistivity values and layer thicknesses indicate a heterogeneous subsurface, where the granitic terrain exhibits better groundwater potential compared to the metasedimentary (quartzite/schist) environment, particularly in areas with significant overburden thickness and extensive fracturing.

The geoelectrical sections revealed four to five distinct subsurface layers, comprising topsoil, clayey laterite, weathered basement, fractured basement, and in some instances, fresh basement. The highest groundwater potential is associated with zones where thick weathered layers and fractured basement units coincide, as these formations enhance porosity and permeability, making them suitable for groundwater storage and extraction. The isopach maps of overburden and fractured basement further validated these findings, highlighting regions with the greatest groundwater prospects.

The results of this study are of significant importance for sustainable groundwater development and management in Mashiji and surrounding areas. The delineation of aquifer zones can aid borehole drilling operations, reducing the risk of failed wells and optimizing groundwater extraction. Additionally, understanding the hydrogeological framework of the area contributes to better planning and implementation of water

supply projects, particularly in regions facing water scarcity. Future research should incorporate additional geophysical techniques such as electromagnetic and seismic methods to complement resistivity surveys, ensuring a more comprehensive assessment of groundwater resources. Furthermore, hydrochemical and hydrological studies should be conducted to evaluate water quality and recharge dynamics, which are crucial for long-term water sustainability in the region. In conclusion, the study has demonstrated that electrical resistivity techniques, particularly VES, remain a reliable and effective tool for groundwater exploration in basement complex terrains. The findings provide a scientific basis for informed decision-making in groundwater resource management, ultimately contributing to improved water availability for the residents of Mashiji and its environs.

REFERENCES

Aboh, H.O., 2001. Detailed Regional Geophysical Investigation of the Subsurface Structures in Katsina Area. Nigeria. Unpublished PhD Thesis. A.B.U. Zaria.

Ajibade, A.C., Wright, J.B., 1989. The Togo-Benin-Nigeria shield: Evidence of crustal aggregation in Pan-African Belt. Tectonophysics, 155, Pp. 125–129.

Alabi, A.A., Bello, R., Ogunghe, A.S., Oyerinde, H.O., 2010. Determination of groundwater potential in Lagos State University, Ojo; using geo-electric methods (Vertical electrical sounding and horizontal profiling), 2 (5), Pp. 68-75.

Al-Garni, M.A., 2009. Geophysical Investigations for Groundwater in a Complex Subsurface Terrain, Wadi Fatima.

Alisiobi, A.R., and Ako, B.D., 2012. Groundwater Investigation Using Combined Geophysical Methods. Search and Discovery Article No. 40914, AAPG Annual Convention and Exhibition, Long Beach, California.

Ariyo, S.O., 2005. Geoelectrical characterization of aquifers and geochemical Study of groundwaters in the basement complex/sedimentary Transition Zone around Ishara, South-Western Nigeria. M. Phil. Thesis. University Of Ibadan, Ibadan, Nigeria.

Bafor, B.E., 1981. The occurrence of sulphide mineralization in the Egbe area of Southwestern Nigeria. Journal of Mining and Geology, 18 (1), Pp. 175-197.

Bala, A.E., Ike, E.C., 2001. The aquifer of the crystalline basement rocks in Gusau area, Northwestern Nigeria. Journal of Mining Geolog., 37 (2), Pp. 177-184.

Danbatta, U.A., 2001. Tectono-metamorphic evolution of the Kazaure Schist Belt, NW Nigeria. Paper presented at the-37" Annual Conference of Nigerian Mininig and Geoscience Society. NMGS Abtract., 33, Pp. 56-109.

Grant, N.K., 1978. Structural distinction between a metasedimentary cover and an underlying basement in the 600 my old Pan-African domain of Northwestern Nigeria. Geol. Soc. Am. Bull., 89, Pp. 50-58.

Holt, R.W., 1982. The geotectonic evolution of the Anka Belt in the Precambrian basement complex of NW Nigeria, PhD dissertation, Open University, Milton Keynes, UK. Pp. 123-128.

Kwari, W.J., 2015. Groundwater quality assessment: a case study of groundwater from hand dug wells in Hawul local Government area of Borno state. Int. jour. Of adv. Res., 3 (2). (ISSN 2320-5407). www.journal-jar.com. Pp537-546.

McCurry, P., 1971. Pan-African orogeny in Northern Nigeria. Geological Society of America Bulletin., 82 (11), Pp. 3251-3262.

McCurry, P., 1979. The Geology of the Precambrian to Lower Palaeozoic Rocks of Northern Nigeria–A Review. In: Kogbe CA, editor. Geology of Nigeria. Lagos: Elizabethan Publishers.

Nur, A., and Ayuni, K.N., 2011. Hydro-geophysical study of Michika and Environs, Northeast Nigeria. International Journal of the Physical Sciences, 6 (34), Pp. 7816-7827.

Nur, A., Kujir, A.S., 2006. Hydro-geoelectrical Study in the North-eastern part of Adamawa State, Nigeria. J. Environ. Hydrol., 14 (19).

Obuobie, E., and Barry, B., 2010. Groundwater in sub-Saharan Africa, Ghana. County Status on Groundwater, Pp. 20.

Oladunjoye, M., Jekayinfa, S., 2015. Efficacy of Hummel (Modified Schlumberger) Arrays of Vertical Electrical Sounding in Groundwater Exploration: Case Study of Parts of Ibadan Metropolis, Southwestern Nigeria. Hindawi Publishing Corporation. Int. J. Geoph., Pp. 124.

Olawuyi, A.K., Abolarin, S.B., 2013. Evaluation of vertical electrical sounding method for groundwater development in basement complex terrain of west-central Nigeria. Nigerian Journal of Technological Development, 10 (2), Pp. 22-28.

Ologe, O., Bankole, S.A., Adeoye, T.O., 2014. Geo-Electric Study for Groundwater Development in Ikunri Estate, Kogi West, Southwestern Nigeria. Ilorin Journal of Science, 1, Pp. 154-166.

Olorunfemi, M.O., and Fasuyi, S.A., 1993. Aquifer types and the geoelectic/ hydrogeological characteristics of part of the central Basement terrain of Nigeria (Niger State). Journal African Earth Science, 16, Pp. 309 – 317.

Oluwa, 1967. Preliminary investigation of groundwater condition in Zaria sheet 102SW. G.S.N. Report. 1462 Bulletin, Pp. 27.

Shuaibu, A.M., 2024. Application of Combined Geoelectrical Techniques for Groundwater Exploration at Federal University Gusau, Zamfara and its Environ, Northwest Nigeria. UMYU Scientifica, 3 (4), Pp. 244 – 259. https://doi.org/10.56919/usci.2434.019.

Shuaibu, A.M., Garba, M.L., and Abubakar, I.Y., 2022. Geoelectrical Assessment of Groundwater Potential within Zamfara and its Environs, Northwestern Nigeria. CaJoST, 1, Pp. 54-70.